Miniature inverted-repeat transposable elements mobilize diverse antibiotic resistance genes in *Enterobacteriaceae*

Ryota Gomi[a,b,*] and Hirokazu Yano[c]

[a]Research Center for Water Environment Technology, School of Engineering, The University of Tokyo, Bunkyo-ku, Tokyo, Japan

[b]Department of Environmental Engineering, Graduate School of Engineering, Kyoto University, Katsura, Nishikyo-ku, Kyoto 615-8540, Japan

[c]Antimicrobial Resistance Research Center, National Institute of Infectious Diseases, Japan Institute for Health Security, Higashimurayama, Tokyo, Japan

[*]Corresponding author: gomi@env.t.u-tokyo.ac.jp, gomi.ryota.34v@kyoto-u.jp

Running title: Composite transposon-like structures bounded by MITEs

ABSTRACT

Miniature inverted-repeat transposable elements (MITEs) are nonautonomous mobile genetic elements (MGEs) that can be mobilized by transposases provided by the relevant autonomous MGEs. Composite transposon-like structures bounded by two MITE copies, designated MITE-COMPs, were previously shown to mobilize the intervening sequences. However, their association with antibiotic-resistance genes (ARGs) has not yet been systematically studied, and only a few MITE-COMP structures with ARGs have been reported to date. This study thus aimed to identify new MITE-COMP members containing ARGs in the genomic sequences of the clinically important bacterial family *Enterobacteriaceae* in public databases. MITE-COMPs were first searched for in the PLSDB database, focusing on small plasmids, using a self-against-self blastn approach. Then, newly and previously identified MITEs were searched for in the NCBI core nucleotide database to identify MITE-COMPs located on other replicons. Bioinformatics analyses identified multiple previously unreported MITE-COMP structures containing ARGs, which are bounded by directly or inversely oriented MITEs, including IS*101*, MITESen1, and a novel 244-bp MITE termed MITE244. All these MITEs seem to have originated from transposons of the Tn*3* family. MITE244 contains a putative cointegrate resolution site related to Tn*21*, and MITE244 copies in MITE-COMPs were

34 predominantly found in inverse orientation. The ARGs embedded in newly identified
35 MITE-COMPs include *bla*$_{KPC-2}$, *qnrS1*, *tet*(A), *qnrD1*, and *floR*. Notably, the *bla*$_{KPC-2}$
36 carbapenemase gene was found in MITE-COMPs bounded by MITE244 and another
37 MITE-COMP bounded by IS*101*. These findings highlight a potential role for MITEs in
38 the spread of diverse ARGs in *Enterobacteriaceae*.
39
40 **IMPORTANCE**
41 Miniature inverted-repeat transposable elements (MITEs) are genetic elements that are
42 mobilized by transposases provided in *trans*. Pairs of MITEs can form composite
43 transposon-like structures (named MITE-COMPs) and can transpose the intervening
44 region in the presence of relevant transposases. Thus, MITE-COMPs can theoretically
45 mediate the spread of antibiotic resistance genes (ARGs). However, only a few MITE-
46 COMP structures with ARGs have been reported to date, probably due to difficulty in
47 identifying MITEs in genome sequences. Here, we identified multiple previously
48 unreported MITE-COMP structures with ARGs, including the clinically important
49 carbapenemase gene *bla*$_{KPC-2}$, by screening *Enterobacteriaceae* replicon sequences
50 deposited in public databases. This study revealed that MITEs can mobilize diverse ARGs
51 in *Enterobacteriaceae* and highlights the importance of considering MITEs when

52 analyzing the genetic contexts of ARGs.

53

54 **KEYWORDS**

55 antibiotic resistance, mobile genetic element, miniature inverted-repeat transposable

56 element, *Enterobacteriaceae*

57

58 **INTRODUCTION**

59 Antibiotic-resistant bacteria, particularly those with multidrug resistance (MDR), are a
60 global health concern. Bacteria can accumulate antibiotic resistance genes (ARGs) with
61 the help of mobile genetic elements (MGEs), which can often lead to MDR. MGEs are
62 categorized into two types: those mobilizing ARGs from one cell to another cell (i.e.,
63 intercellular mobilization) and those mobilizing ARGs from one replicon to another
64 replicon or to different locations within the same replicon (i.e., intracellular
65 mobilization).[1] Intercellular mobilization mechanisms such as conjugation can directly
66 contribute to horizontal transfer of ARGs and thus the emergence and spread of MDR.
67 Intracellular mobilization can also contribute to the increase of MDR in multiple ways;
68 for example, by mobilizing ARGs on a plasmid to different plasmids, thereby increasing
69 the potential of the ARGs to be transmitted to additional bacterial recipients via
70 conjugation.[2]

71 MGEs mediating intracellular mobilization of ARGs include well-studied elements such
72 as insertion sequences (ISs) and transposons. These are called autonomous (i.e., capable
73 of self-transposition) elements. On the other hand, there are nonautonomous elements,
74 which can also mediate intracellular mobilization but need the transposase activity
75 provided by autonomous elements in the same cell.[1] Among the known nonautonomous

76 elements are structures called miniature inverted-repeat transposable elements (MITEs).[3]
77 MITEs are thought to have originated from ISs or transposons. They retain the terminal
78 inverted repeats (IRs) but lack the internal regions, including the transposase gene(s).
79 They are typically 50 bp–500 bp in size and create direct repeats (DRs) upon insertion.[4]
80 Composite transposon-like structures bounded by two MITEs, which are defined here as
81 MITE-COMPs, were previously shown to transpose the intervening sequences when
82 transposase activity was provided in *trans*.[5, 6] Therefore, MITEs can act as an ARG
83 mobilization factor when the ARG is embedded within a MITE-COMP structure.
84 However, only a few studies have reported MITE-COMP structures carrying ARGs, even
85 in the clinically important bacterial family *Enterobacteriaceae* (**Figure S1**). These
86 include two MITE-COMP structures bounded by integron mobilization units (IMUs)[5, 7]
87 and a MITE-COMP structure bounded by IS*101*.[8] IMU and IS*101* are MITEs carrying
88 IRs related to Tn*3*-family transposons and thus are classified as Tn*3*-derived inverted-
89 repeat miniature elements (TIMEs).[6] In these cases, the MITE-COMPs were located on
90 small plasmids (<10 kbp).
91 MITEs tend to be overlooked in standard annotation pipelines due to their lack of
92 transposase gene(s). Thus, the contribution of MITEs to the intracellular mobility of
93 ARGs is likely underestimated. Hence, this study aimed to identify previously overlooked

94 MITE-COMPs carrying ARGs in *Enterobacteriaceae* by data-mining. MITE-COMPs
95 were first searched for in the genomes of small plasmids in a public plasmid database.
96 Then, newly identified and previously known MITEs were searched for in the NCBI
97 database to discover MITE-COMP structures in other types of replicons.
98

99 **METHODS**

100 **Plasmid sequences**

101 Plasmid sequences were downloaded from PLSDB (v. 2024_05_31_v2) (n = 72,556).[9]
102 Plasmid sequences meeting the following criteria were extracted: (i) at least one ARG
103 was detected by Abricate (v1.0.1, https://github.com/tseemann/abricate) with the ncbi
104 database;[10] (ii) at least one plasmid replicon was detected by Abricate (v1.0.1) with the
105 plasmidfinder database (this was to exclude sequences that are not likely to be true
106 plasmids);[11] (iii) the length is 20,000 bp or shorter; and (iv) the plasmid host is
107 *Enterobacteriaceae*. Plasmid sequences meeting the above criteria (n = 1,007) were
108 subjected to self-against-self blastn analysis to detect MITE-COMP structures carrying
109 ARGs as described below.

110 **Detection of MITE-COMP structures carrying ARGs**

111 A self-against-self blastn search was performed for each plasmid sequence using
112 makeblastdb (v2.16.0+) and blastn (v2.16.0+) with default parameters. Plasmid
113 sequences with blastn hits meeting the following criteria were retained: (i) the alignment
114 length is between 50 bp and 500 bp; (ii) the percentage of identical matches is 98% or
115 higher; (iii) a sequence longer than 500 bp is present between the aligned part of the query
116 sequence and that of the subject sequence. These criteria were applied to detect repeat
117 sequences (50 bp–500 bp) surrounding a stretch of sequence (> 500 bp) in a plasmid (see
118 **Figure S2** for rationales for these criteria). To confirm that the 50-bp to 500-bp repeat
119 sequences are actually MITEs, a self-against-self blastn search was performed for each
120 repeat sequence to identify IRs, which are the signature of MITEs. The blastn search was
121 performed by using a word size of six to increase the sensitivity, and the result was
122 visualized using CLC Main Workbench 24 (Qiagen, Hilden, Germany) (**Figure S3**). The
123 putative MITE sequences were checked for identity to any known elements in the ISfinder
124 database.[12] To avoid false positives, only MITE-COMP structures flanked by DRs, which
125 are typically created upon insertion of the structure, were considered for further analysis.
126 Plasmids with MITE-COMP structures carrying ARGs were annotated using ISfinder and
127 the blastn web tool (https://blast.ncbi.nlm.nih.gov/Blast.cgi).

128 The MITE(s) found in the above approach, previously described MITEs associated with
129 ARGs in *Enterobacteriaceae* (i.e., IMU and IS*101*),[5, 7, 8] and *Enterobacteriaceae* MITEs
130 listed in the ISfinder database (i.e., MITEKpn1 and MITESen1, excluding MITEEc1,
131 which is an enterobacterial repetitive intergenic consensus [ERIC] sequence), were
132 searched for in the NCBI core nucleotide database (core_nt) using the blastn web tool to
133 identify additional ARG-carrying MITE-COMP structures in *Enterobacteriaceae* (last
134 accessed in July 2025). Replicons with two or more blastn hits with ≥95% identity and
135 ≥95% coverage were manually screened to detect the MITE-COMP structures.

136 **Detection of MITEs in RefSeq *Enterobacteriaceae* genomes**

137 RefSeq *Enterobacteriaceae* genomes with an assembly level of "complete genome" were
138 downloaded using the NCBI Datasets command-line tools (v18.9.0) in October 2025 (n
139 = 11,572).[13] MITEs identified as being associated with ARGs were searched for in the
140 retrieved genomes using makeblastdb (v2.16.0+) and blastn (v2.16.0+) with default
141 parameters. We used the same criteria as the online blastn search to define the presence
142 of MITE sequences (i.e., ≥95% identity and ≥95% coverage).

143

144 **RESULTS AND DISCUSSION**

145 **Identification of MITE-COMP structures carrying ARGs**

146 First, we conducted self-against-self blastn analysis to identify putative MITE-COMP
147 structures in small *Enterobacteriaceae* plasmids registered in PLSDB. PLSDB is a
148 curated and non-redundant plasmid database sourced from the NCBI database.[9] This
149 relatively small dataset made manual curation of the blastn results feasible, which
150 includes confirmation of the IRs in putative MITEs and DRs flanking the entire MITE-
151 COMP structures. These procedures revealed MITE-COMP structures carrying ARGs in
152 six plasmids (**Table S1**). One of these plasmids was pKFu015_4 (NZ_CP147134), which
153 was previously reported to carry the IS*101*-based MITE-COMP containing *qnrD1*.[8] The
154 remaining five plasmids contain the same MITE-COMP structure with $bla_{\text{KPC-2}}$ and a
155 truncated bla_{TEM} gene, which is bounded by two copies of a 244-bp MITE (hereafter
156 named MITE244). Plasmids pCHE-A (NC_012006) and pCHE-A1 (NZ_KX244760),
157 which were previously reported to contain IMU-based MITE-COMPs, were detected by
158 the self-against-self blastn searches but were filtered out in manual curation, because the
159 MITE-COMP structures in these plasmids are not flanked by DRs.[5, 7]
160 To identify MITE-COMP structures in small plasmids not indexed in PLSDB, in longer
161 plasmids, and also in chromosomes, we performed online blastn searches using MITE244
162 and previously reported MITEs (IS*101*, IMU, MITEKpn1, and MITESen1) as query
163 sequences (see **Table S2** for the sequence of each MITE). This online blastn analysis

164 identified 141 additional replicons carrying MITE-COMPs with ARGs. These included
165 136 plasmids and one chromosome carrying MITE244-based MITE-COMPs (most of
166 which contain *tet*(A)), one plasmid carrying an IS*101*-based MITE-COMP, and three
167 plasmids carrying MITESen1-based MITE-COMPs (**Table S1**).
168 The genetic contexts of MITE-COMPs identified using the above approaches were
169 thoroughly analyzed as described below.

170 **MITE-COMPs bounded by two copies of MITE244**

171 As mentioned above, we detected MITE244-based MITE-COMPs in a total of 142
172 replicons (i.e., five identified by the self-against-self blastn analysis and 137 identified by
173 the online blastn analysis). Roughly, three types of MITE244-based MITE-COMPs were
174 identified. One of them is a MITE-COMP structure carrying bla_{KPC-2} and a truncated
175 bla_{TEM} gene, which is bounded by directly oriented MITE244 copies (**Figure 1A**). This
176 genetic context was previously described as a variant of non-Tn*4401* elements (NTE_{KPC}),
177 NTE_{KPC}-IId; however, the authors did not mention the presence of MITEs at its boundaries
178 (they addressed the presence of 243-bp, not 244-bp, repeats at its boundaries though).[14]
179 This MITE-COMP was detected in one Col-like plasmid and six highly related IncQ1
180 plasmids (**Table S1**). Analysis of the sequences flanking the MITE-COMPs revealed that
181 there is one insertion location with unique DRs per replicon type (**Figure 1B** and **Table**

182 **S1**), totaling two unique transposition events. In the Col-like plasmid pKPC45a, NTE_{KPC}-
183 IId is inserted in a gene encoding an endonuclease-family protein found in pRJKP36-5-
184 like plasmids, creating 5-bp DRs of TATAT. In the IncQ1 plasmids (e.g., pKQPS142b),
185 NTE_{KPC}-IId is inserted in an intergenic region found in p4-N2251932-like plasmids,
186 creating 6-bp DRs of TGTTTA. In one of the IncQ1 plasmids, pKPN535a, three copies
187 of MITE244 are present, and a sequence identical to pSYCC1_6 is present between two
188 of the MITE244 copies. This indicates a cointegrate formation by "paste-and-copy"
189 transposition of MITE244 or homologous recombination between two MITE244 copies,
190 leading to the fusion of a pKQPS142b-like plasmid and pSYCC1_6.
191 Another MITE244-based MITE-COMP, which contains *qnrS1* and is bounded by
192 inversely oriented MITE244 copies, was detected in two untypeable plasmids, pK814-
193 QNRS and pK1326-qnrS (**Figure 1A and 1B**). In these plasmids, the MITE-COMP
194 structure is inserted in the same position in the intergenic region found in a pCP102-like
195 plasmid with 5-bp DRs of ATCCA; therefore, a total of one unique transposition event
196 was detected. Sequence comparison indicates that acquisition of a 35-kbp phage-like
197 region by a pK814-QNRS-like plasmid led to the generation of pK1326-qnrS.
198 We detected a *tet*(A)-carrying MITE244-based MITE-COMP (or its variants) in 133
199 replicons (**Table S1**). This MITE-COMP structure contains a partial sequence of Tn*1721*,

200 which is bounded by inversely oriented MITE244 copies (**Figure 1A**).[15] This MITE-
201 COMP structure was inserted in a total of three unique locations: a gene encoding a
202 DUF6710-family protein (DRs of AGCAA, n = 114), a gene encoding a hypothetical
203 protein (DRs of TATAA, n = 18), and a gene encoding an IS*1*-family transposase (DRs of
204 TACTT, n = 1) (**Figure 1C** and **Table S1**). This indicates that three independent
205 transposition events of this MITE-COMP structure had occurred in the past. In 114
206 replicons with DRs of AGCAA, two types of the MITE-COMP were identified: one with
207 an inverted internal structure (n = 52) and the other without (n = 62) (see below for more
208 detailed discussion). Furthermore, there were several In/Del variations within the MITE-
209 COMP structure, two of which involved alterations of ARG contents (**Table S1** and
210 **Figure S4**). In p1_A24352 (CP181749), a resistance region containing $bla_{\text{TEM-1B}}$ and
211 $bla_{\text{CTX-M-206}}$ is inserted within the left MITE244 copy. In pEC224_KPC (CP018945), the
212 Tn*1721* fragment is partially deleted and replaced with a truncated Tn*3*-like transposon
213 and a truncated Tn*4401*-like transposon containing $bla_{\text{KPC-2}}$.[16] In these cases, the DR
214 sequences flanking the MITE-COMPs are the common ones (AGCAA); thus the In/Del
215 variations were likely introduced after the insertion of the original MITE-COMP carrying
216 *tet*(A). The outermost IRs within the altered MITE-COMP structures are intact, implying

217 the feasibility of further transposition if the relevant transposase activity is provided in

218 *trans* (**Figure S4**).

219 **A MITE-COMP bounded by two copies of IS*101***

220 We identified a previously unreported IS*101*-based MITE-COMP structure in one

221 *Enterobacter kobei* IncX3 plasmid, pEkFL23_IncX3 (**Figure 2A**). This MITE-COMP is

222 bounded by inversely oriented IS*101* copies and carries $bla_{\text{KPC-2}}$ embedded within a

223 truncated Tn*4401b* structure.[16] This genetic context was previously reported as Tn*4401k*,

224 but the presence of IS*101* elements was not addressed in the previous study.[17] The

225 sequence between the two IS*101* elements in this MITE-COMP corresponds to the partial

226 sequence of plasmids such as pKPC_FCF/3SP. The sequence of pEkFL23_IncX3, except

227 for the MITE-COMP, is highly similar to multiple *Enterobacteriaceae* plasmids (e.g., p3-

228 N4292977). Thus, pEkFL23_IncX3 may have been generated by IS*101*-mediated

229 transposition of the partial pKPC_FCF/3SP sequence into a p3-N4292977-like plasmid

230 (**Figure 2B**). The presence of 5-bp DRs (ATTCT) flanking the MITE-COMP supports

231 this idea.

232 **MITE-COMPs bounded by two copies of MITESen1**

233 We identified two different MITESen1-based MITE-COMPs in the same location with

234 the same flanking 5-bp DRs (TAATA) in two IncX1-IncX2 hybrid plasmids, pLAO96 and

235 pSC-KP585-2 (**Figure 3A** and **3B**). One MITE-COMP contains *qnrS1*, and the other
236 contains *floR*. MITESen1 copies are directly oriented in these MITE-COMPs.
237 Interestingly, there are IncX1-X2 hybrid plasmids carrying a single MITESen1 copy
238 inserted in the same location (e.g., pCUWW06A). We speculate that pLAO96 and pSC-
239 KP585-2 were generated by integration of a hypothetical circular molecule containing
240 MITESen1 and an ARG into a pCUWW06A-like plasmid already carrying a single copy
241 of MITESen1 (**Figure 3B**). The hypothetical circular molecules might be generated by
242 (i) homologous recombination between directly oriented MITESen1, (ii) a transposase-
243 dependent mechanism similar to IS*26* translocatable unit (TU) formation,[18] or (iii) TnpR-
244 dependent site-specific recombination if MITESen1 possesses a cointegrate resolution
245 site *res* (also see **Figure S5** for another possible pathway for generation of the *floR*-
246 containing circular element). Integration of the circular molecule might occur by
247 homologous recombination between MITESen1 copies or a transposase-dependent TU
248 incorporation-like mechanism.[19]
249 A plasmid with the repE(pEh60-7) replicon, pECC-003-1, was found to carry a remnant
250 of a MITESen1-based MITE-COMP containing *qnrD1* (**Figure 3A** and **3B**). In pECC-
251 003-1, the MITE-COMP structure is interrupted by an IS*26* element at the left MITESen1.
252 The remaining MITESen1 is present in the plasmid next to another inversely oriented

253 IS*26* element. This arrangement is consistent with intramolecular replicative transposition

254 (in *trans*) of an IS*26* element into MITESen1 in the intact MITE-COMP structure.[20] The

255 presence of an 8-bp DR (ATATCAAC) next to each IS*26* element on the MITESen1-sides

256 supports this, though the intact version of this MITE-COMP structure was not present in

257 the NCBI core_nt database.

258 **Characteristic features of MITE244**

259 All MITEs forming the MITE-COMP structures identified in the present study (i.e.,

260 MITE244, IS*101*, and MITESen1) carry IRs related to Tn*3*-family transposons (**Figure**

261 **4A**). Thus, these MITEs are classified as TIMEs.[6] IRs of MITE244 and the previously

262 reported IMU show more similarities to IRs of Tn*21* than to those of Tn*3*, IS*101*, TIME2,[6]

263 and MITESen1. Thus, MITE244 and IMU seem to have originated from the Tn*21*

264 subgroup of the Tn*3* family.[21] IS*101* possesses the functional internal cointegrate

265 resolution site *res*.[22] To determine whether MITE244 contains a *res* site, we aligned the

266 MITE244 internal sequence and the experimentally determined *res* sites of Tn*21* and

267 Tn*1721* (**Figure 4B**).[23] The *res* sites of the Tn*3* family consist of three subsites (site I, site

268 II, and site III) where TnpR dimers bind. Strand exchange takes place at the center of site

269 I when *res* sites are directly oriented in the same molecule.[21] The MITE244 internal

270 sequence shows similarity to both Tn*21 res* and Tn*1721 res* at all three subsites. Therefore,

271 we speculate that MITE244 contains a functional *res* site of the Tn*21* subgroup. On the
272 other hand, the internal sequence of IMU is extensively diverged from the *res* sequence
273 of the Tn*21* subgroup, which hindered the determination of whether IMU contains a *res*
274 site or not.
275 In principle, the functionality of *res* affects the stability of the MITE-COMP structure.
276 When MITE244 copies are directly oriented within MITE-COMPs, the segment between
277 two *res* sites can be deleted in the presence of TnpR. On the other hand, when MITE244
278 copies are inversely oriented, the segment between two *res* sites can be inverted by TnpR
279 *in vivo*.[24,25] Among 142 replicons containing MITE244-based MITE-COMPs, only seven
280 replicons contain directly oriented MITE244 copies, while 135 replicons contain
281 inversely oriented MITE244 copies (**Table S1**). This orientation bias is consistent with
282 the idea that MITE-COMPs carrying directly repeated MITE244 copies are structurally
283 unstable due to the intrinsic resolution activity in the presence of Tn*21*-related TnpR. On
284 the other hand, the most prevalent MITE-COMPs in the present study, namely MITE-
285 COMPs with *tet*(A), carry MITE244 copies in inverse orientation. As noted above, the
286 MITE-COMP structures of the 114 replicons with DRs of AGCAA are classified into
287 those with an inverted internal structure (n = 52) and those without (n = 62) (**Figure 1C**
288 **and 4C**). This inversion could be explained by TnpR-mediated site-specific

289 recombination at the *res* sites rather than by homologous recombination between
290 inversely oriented MITE244 copies, given the short length of MITE244. Because
291 MITE244 contains a putative *res* site, the transposition of MITE244-based MITE-COMPs
292 with inversely oriented MITE244 copies should follow a two-step process: cointegrate
293 formation and cointegrate resolution in the presence of Tn*21*-related transposons (**Figure**
294 **4D**). Cointegrate resolution can occur by RecA-dependent homologous recombination or
295 site-specific recombination involving Tn*21*-related TnpR and *res* sites.

296 **Prevalence of MITEs in RefSeq *Enterobacteriaceae* genomes**

297 The NCBI core_nt database, which we used in the online blastn analysis, contains a
298 mixture of complete genomes and sequences that are not derived from complete genomes
299 (e.g., plasmid sequences without the host chromosomal sequences), preventing the
300 accurate estimation of the prevalence of MITEs in *Enterobacteriaceae* genomes. Thus,
301 we retrieved RefSeq complete *Enterobacteriaceae* genomes (n = 11,572) and detected
302 MITEs in these genomes to avoid this problem. The frequency of genomes carrying each
303 MITE was as follows: MITE244 (n = 109, 0.94%), IS*101* (n = 49, 0.42%), MITESen1 (n
304 = 264, 2.28%), and IMU (n = 7, 0.06%) (**Table S3**). The frequency of genomes with a
305 replicon(s) carrying multiple copies of each MITE was as follows: MITE244 (n = 71,
306 0.61%), IS*101* (n = 4, 0.03%), MITESen1 (n = 54, 0.47%), and IMU (n = 2, 0.02%). In

307 total, 408 genomes (3.53%) carried at least one of these MITEs, indicating these MITEs
308 are rare but present at a detectable frequency. Interestingly, these MITEs were
309 predominantly detected in plasmids (n = 444, 97.16%) and very rarely in chromosomes
310 (n = 13, 2.84%).

311 **Study limitations**

312 This study has limitations. First, the self-against-self blastn approach, which allows *de*
313 *novo* identification of MITEs that form MITE-COMP structures, was performed only on
314 small plasmids (<20 kbp). Thus, novel MITEs potentially present in other types of
315 replicons might have been missed. Performing the self-against-self blastn analysis also
316 on large plasmids and chromosomes may enable the identification of more MITE
317 elements; however, this approach is unwieldly because it will return exponentially more
318 blastn hits, which makes manual curation of the results (e.g., confirmation of DRs at the
319 ends) almost impossible. A direction for future work would be to develop software for
320 automated detection of MITE-COMP structures. A second limitation of this study is that
321 MITE-COMPs were detected only in *Enterobacteriaceae*. Although rare, there seem to
322 be MITE-COMP structures containing ARGs in other bacteria as well, such as
323 *Acinetobacter* spp.[26] Extending the approach employed in the present study to other
324 bacteria may uncover additional MITE-COMP elements.

Conclusions

The present study identified multiple previously unreported MITE-COMPs containing ARGs, which are bounded by three types of MITEs (i.e., MITE244, IS*101*, and MITESen1). These three MITEs and also IMU are all categorized as TIMEs, but they are divergent and seem to have independently emerged from distinct transposons of the Tn*3* family. Interestingly, the same MITEs were associated with different ARGs, and the same ARGs were associated with different MITEs. This study revealed that MITEs contribute to the intracellular mobilization of diverse ARGs in *Enterobacteriaceae* and highlights the importance of taking these elements into account when analyzing the genetic contexts of ARGs.

Acknowledgments

This work was supported by JSPS KAKENHI (grant number JP22K18038) and the Environment Research and Technology Development Fund (JPMEERF20235R01) of the Environmental Restoration and Conservation Agency, provided by the Ministry of the Environment of Japan. Computations were partially performed on the NIG supercomputer at ROIS National Institute of Genetics.

Author contributions

Conceptualization: R.G. Methodology: R.G. Formal analysis: R.G. and H.Y. Data Curation: R.G. Visualization: R.G. and H.Y. Project administration: R.G. Funding acquisition: R.G. Writing - Original Draft: R.G. and H.Y. Writing - Review & Editing: R.G. and H.Y.

REFERENCES

1. Partridge SR, Kwong SM, Firth N, Jensen SO. Mobile Genetic Elements Associated with Antimicrobial Resistance. *Clin Microbiol Rev* 2018; **31**.
2. Lerminiaux NA, Cameron ADS. Horizontal transfer of antibiotic resistance genes in clinical environments. *Can J Microbiol* 2019; **65**: 34-44.
3. Delihas N. Impact of small repeat sequences on bacterial genome evolution. *Genome Biol Evol* 2011; **3**: 959-73.
4. Minnick MF. Functional Roles and Genomic Impact of Miniature Inverted-Repeat Transposable Elements (MITEs) in Prokaryotes. *Genes (Basel)* 2024; **15**.
5. Poirel L, Carrer A, Pitout JD, Nordmann P. Integron mobilization unit as a source of mobility of antibiotic resistance genes. *Antimicrob Agents Chemother* 2009; **53**: 2492-8.
6. Szuplewska M, Ludwiczak M, Lyzwa K et al. Mobility and generation of mosaic non-autonomous transposons by Tn*3*-derived inverted-repeat miniature elements (TIMEs). *PLoS One* 2014; **9**: e105010.
7. Pedersen T, Sekyere JO, Govinden U et al. Spread of Plasmid-Encoded NDM-1 and GES-5 Carbapenemases among Extensively Drug-Resistant and Pandrug-Resistant Clinical *Enterobacteriaceae* in Durban, South Africa. *Antimicrob Agents Chemother* 2018; **62**.
8. Gomi R, Adachi F. Quinolone Resistance Genes *qnr*, *aac(6')-Ib-cr*, *oqxAB*, and *qepA* in Environmental *Escherichia coli*: Insights into Their Genetic Contexts from Comparative Genomics. *Microb Ecol* 2025; **88**: 6.
9. Molano LG, Hirsch P, Hannig M et al. The PLSDB 2025 update: enhanced annotations and improved functionality for comprehensive plasmid research. *Nucleic Acids Res* 2025; **53**: D189-D96.
10. Feldgarden M, Brover V, Gonzalez-Escalona N et al. AMRFinderPlus and the Reference Gene Catalog facilitate examination of the genomic links among antimicrobial resistance, stress response, and virulence. *Sci Rep* 2021; **11**: 12728.
11. Carattoli A, Zankari E, Garcia-Fernandez A et al. In silico detection and typing of plasmids using PlasmidFinder and plasmid multilocus sequence typing. *Antimicrob Agents Chemother* 2014; **58**: 3895-903.
12. Siguier P, Perochon J, Lestrade L et al. ISfinder: the reference centre for bacterial insertion sequences. *Nucleic Acids Res* 2006; **34**: D32-6.
13. O'Leary NA, Cox E, Holmes JB et al. Exploring and retrieving sequence and metadata for species across the tree of life with NCBI Datasets. *Sci Data* 2024; **11**: 732.
14. Cerdeira LT, Lam MMC, Wyres KL et al. Small IncQ1 and Col-Like Plasmids Harboring bla_{KPC-2} and Non-Tn*4401* Elements (NTE_{KPC}-IId) in High-Risk Lineages of *Klebsiella pneumoniae* CG258. *Antimicrob Agents Chemother* 2019; **63**.

385 15. Allmeier H, Cresnar B, Greck M, Schmitt R. Complete nucleotide sequence of Tn*1721*:
386 gene organization and a novel gene product with features of a chemotaxis protein. *Gene* 1992;
387 **111**: 11-20.
388 16. Naas T, Cuzon G, Villegas MV et al. Genetic structures at the origin of acquisition of
389 the beta-lactamase bla_{KPC} gene. *Antimicrob Agents Chemother* 2008; **52**: 1257-63.
390 17. Guardatti RGM, Kraychete GB, Picao RC. Analysis of distinct bla_{KPC}-encoding
391 plasmids in an *Enterobacter kobei* strain recovered from recreational coastal water. *Sci Total*
392 *Environ* 2024; **915**: 169945.
393 18. Harmer CJ, Hall RM. IS*26*-Mediated Precise Excision of the IS*26-aphA1a*
394 Translocatable Unit. *mBio* 2015; **6**: e01866-15.
395 19. Harmer CJ, Moran RA, Hall RM. Movement of IS*26*-associated antibiotic resistance
396 genes occurs via a translocatable unit that includes a single IS*26* and preferentially inserts
397 adjacent to another IS*26*. *mBio* 2014; **5**: e01801-14.
398 20. He S, Hickman AB, Varani AM et al. Insertion Sequence IS*26* Reorganizes Plasmids in
399 Clinically Isolated Multidrug-Resistant Bacteria by Replicative Transposition. *mBio* 2015; **6**:
400 e00762.
401 21. Nicolas E, Lambin M, Dandoy D et al. The Tn*3*-family of Replicative Transposons.
402 *Microbiol Spectr* 2015; **3**.
403 22. Ishizaki K, Ohtsubo E. Cointegration and resolution mediated by IS*101* present in
404 plasmid pSC101. *Mol Gen Genet* 1985; **199**: 388-95.
405 23. Rogowsky P, Halford SE, Schmitt R. Definition of three resolvase binding sites at the
406 *res* loci of Tn*21* and Tn*1721*. *EMBO J* 1985; **4**: 2135-41.
407 24. Droge P, Cozzarelli NR. Recombination of knotted substrates by Tn*3* resolvase. *Proc*
408 *Natl Acad Sci U S A* 1989; **86**: 6062-6.
409 25. Yano H, Garruto CE, Sota M et al. Complete sequence determination combined with
410 analysis of transposition/site-specific recombination events to explain genetic organization of
411 IncP-7 TOL plasmid pWW53 and related mobile genetic elements. *J Mol Biol* 2007; **369**: 11-26.
412 26. Zong Z. The complex genetic context of bla_{PER-1} flanked by miniature inverted-repeat
413 transposable elements in *Acinetobacter johnsonii*. *PLoS One* 2014; **9**: e90046.
414
415

416 **Figures**

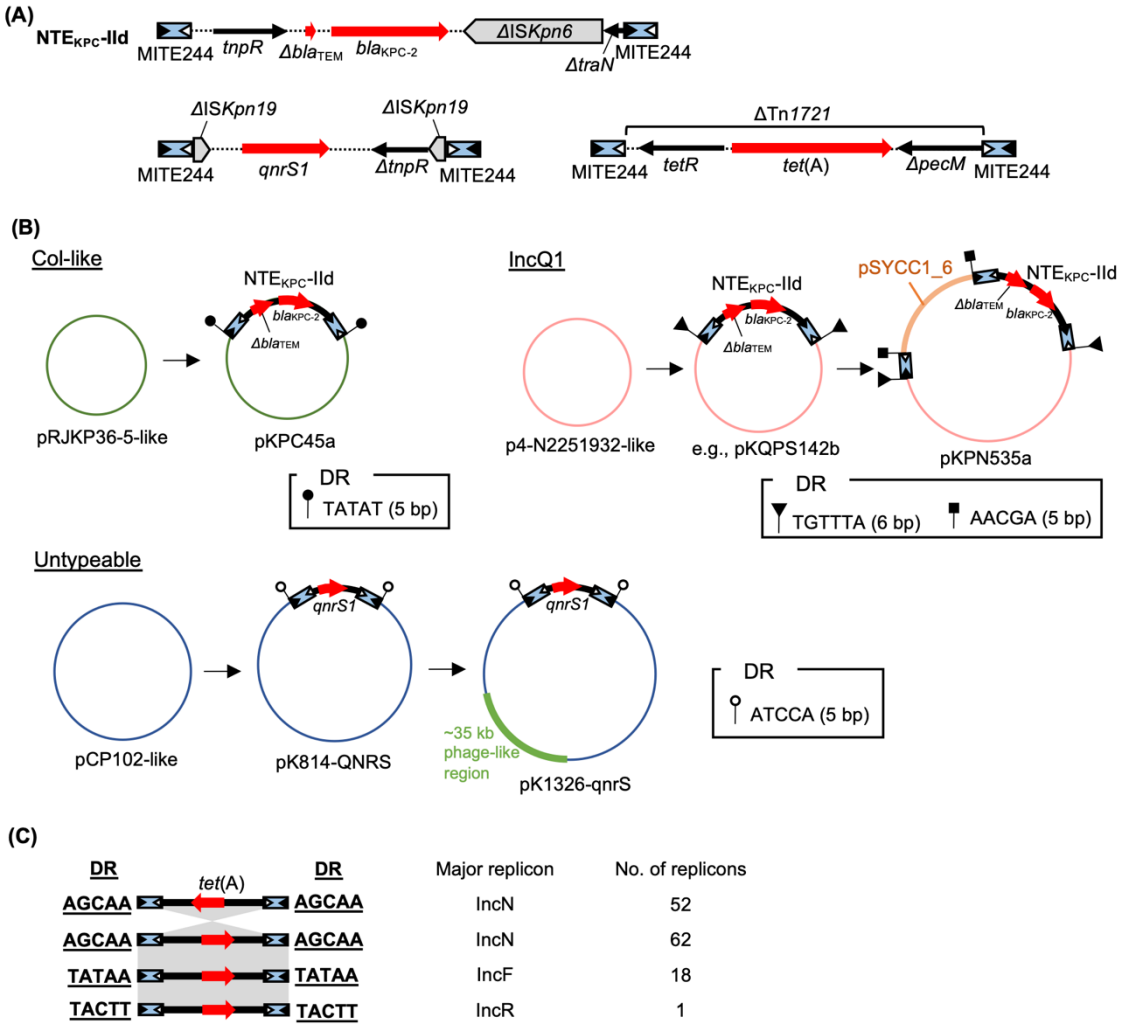

417

418 **Figure 1**. (A) MITE-COMP structures bounded by MITE244. Red arrows indicate
419 ARGs, gray pointed boxes indicate ISs, blue boxes indicate MITEs, and black arrows
420 indicate other genes. The left IR (IRL) is indicated by a black triangle, and the right IR
421 (IRR) is indicated by a white triangle within each MITE. (B) Plasmids carrying
422 MITE244-based MITE-COMP structures. For each MITE-COMP structure, only MITEs
423 and ARGs are depicted for brevity. DRs are shown as differently shaped flags, and their
424 sequences are shown in boxes. The accession numbers of the plasmids are as follows:
425 pRJKP36-5, CP100081; pKPC45a, MH595534; p4-N2251932, CP165866;
426 pKQPS142b, CP023480; pKPN535a, MH595533; pSYCC1_6, CP113183; pCP102,
427 CP104015; pK814-QNRS, CP183858; and pK1326-qnrS, CP183864. (C) DRs of
428 MITE-COMPs carrying *tet*(A). Major replicon types and the numbers of replicons are
429 shown on the right side.

430

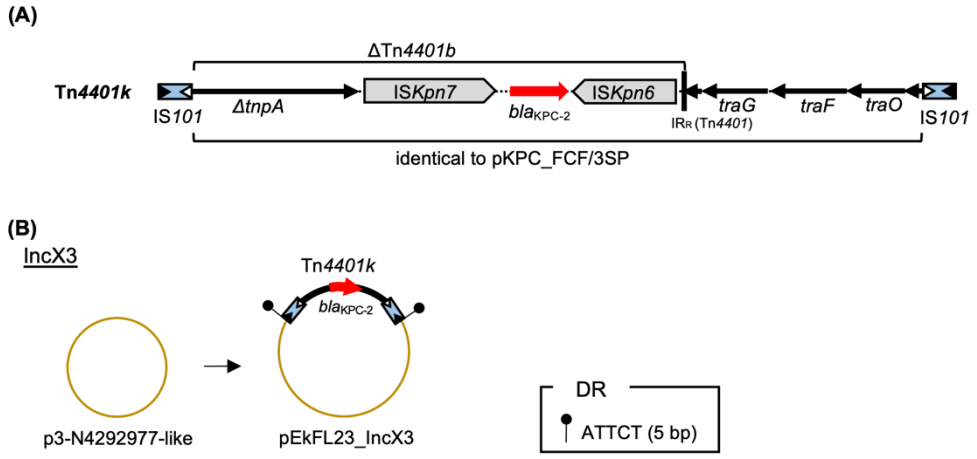

Figure 2. (A) IS*101*-based MITE-COMP structure carrying bla_{KPC-2}. (B) Structure of the plasmid containing the IS*101*-based MITE-COMP. Genes and elements are shown as in **Figure 1**. The accession numbers of the plasmids are as follows: pKPC_FCF/3SP, CP004367; p3-N4292977, CP165819; and pEkFL23_IncX3, OQ434669.

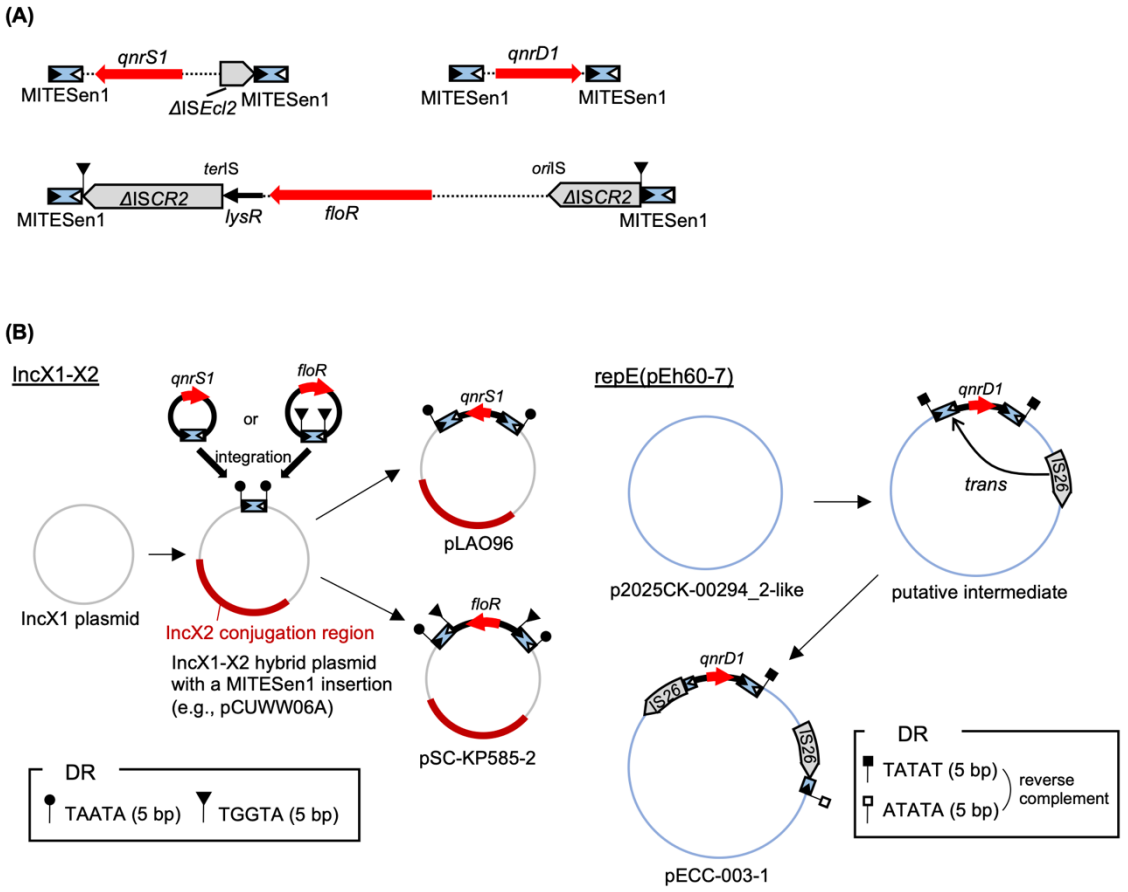

Figure 3. (A) MITE-COMP structures bounded by MITESen1. (B) Plasmids carrying MITESen1-based MITE-COMPs. Genes and elements are shown as in the previous

440 figures. "*trans*" indicates intramolecular replicative transposition (in *trans*) of IS*26*. The
441 accession numbers of the plasmids are as follows: pCUWW06A, CP182140; pLAO96,
442 OP242301; pSC-KP585-2, CP123874; p2025CK-00294_2, CP194151; and pECC-003-
443 1, CP143772.
444

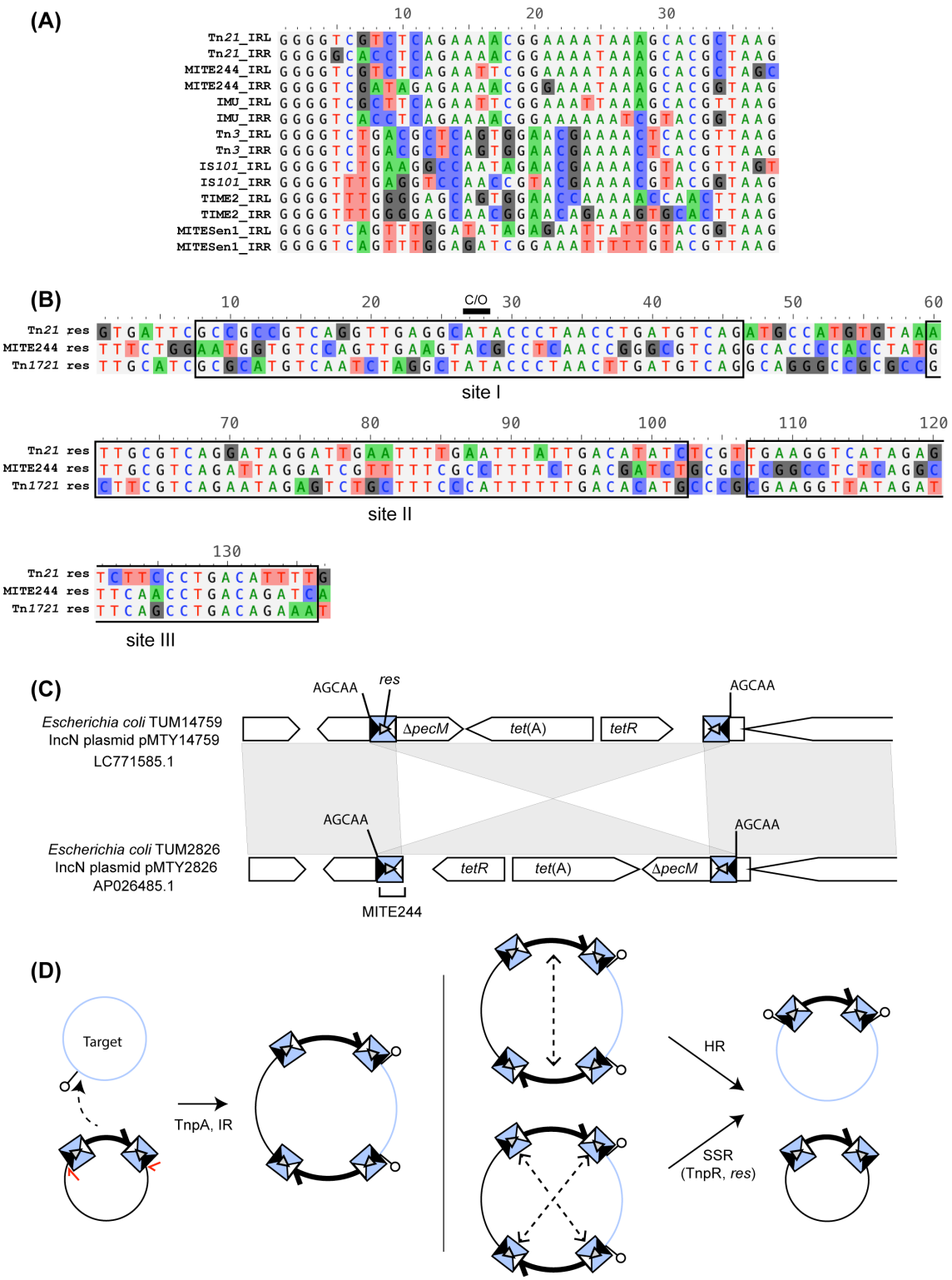

Figure 4. (A) Multiple alignment of IRs of MITEs, Tn*3*, and Tn*21*. (B) Multiple alignment of *res* sites of Tn*21*, MITE244, and Tn*1721*. Definition of subsites follows a previous study.[23] See **Table S2** for the sequences of MITE244, IMU, IS*101*, and MITESen1. The remaining sequences were derived from the following accession

450 numbers: Tn*21*, AF071413; Tn*3*, HM749966; TIME2, KJ920398; and Tn*1721*, X61367.
451 (C) Two frequent forms of MITE244-based MITE-COMPs carrying *tet*(A) inserted in
452 the same location. (D) Deduced transposition pathways of MITE-COMPs bounded by
453 inversely oriented MITE244 copies. Cointegrate formation (left) is mediated by TnpA
454 and IRs, followed by replication. Cointegrate resolution (right) is mediated by RecA-
455 dependent homologous recombination (HR) between duplicated MITE-COMPs or by
456 TnpR/*res*-dependent site-specific recombination (SSR). SSR can occur between either
457 pair of the directly oriented MITE244 copies. Nicking sites in the donor molecule are
458 indicated by red arrows.
459